

^{119}Sn NMR of Alkali Metal Tin Clathrates

Frank Haarmann, Michael Baitinger and Yuri Grin

The clathrate I compounds $M_8\text{Sn}_{44}\text{I}_2$ ($M = \text{K}, \text{Rb}$ and Cs) contain an anionic framework Sn_{44}^{8-} , in which the alkali-metal cations occupy Sn_{20} and Sn_{24} polyhedra (Fig. 1). According to extensive X-ray diffraction studies the Sn framework contains vacancies arising from a merely 66% occupation of the Sn1 site [1]. As structural defects affect the physical properties, the thermoelectricity of $M_8\text{Sn}_{44}\text{I}_2$ compounds differs significantly from that of related compounds like $M_8\text{Si}_{46}$ clathrates with fully occupied framework positions [2]. Since two defect positions per unit cell imply that 8 three-fold bonded Sn3 atoms adjacent to the defects have a clearly different environment compared to the remaining 36 Sn atoms, we analyzed the influence of the structural vacancies by NMR experiments.

The compounds were synthesized from the ele-

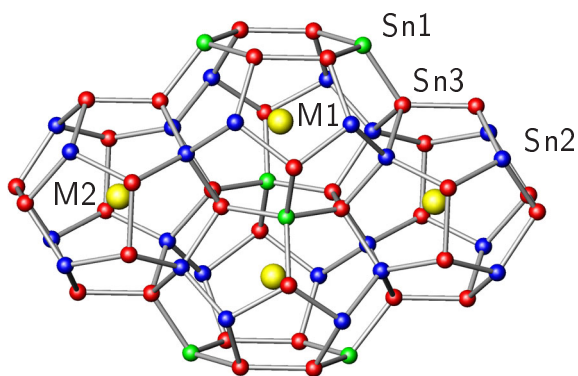


Fig. 1: Section of the clathrate I network containing a pentagondodecahedron around M1 atoms and a tetra-kaiidecahedron around M2 atoms ($M = \text{K}, \text{Rb}, \text{Cs}$).

ments in the stoichiometric ratio using Nb tubes as containers. Though some of the samples showed a slight excess of tin, there was generally no evidence for impurities according to X-ray diffraction measurements, chemical analysis and thermal analysis.

Both ^{117}Sn and ^{119}Sn have a nuclear spin of $I = 1/2$ and therefore only the central transition $-1/2 \leftrightarrow 1/2$ can be observed. Hence, the interpretation is simplified even though complicated NMR spectra can still be obtained. Furthermore, ^{117}Sn and ^{119}Sn

have a small natural abundance of 7.6 % and 8.6 %, respectively.

The static ^{119}Sn NMR spectra obtained at room temperature in a magnetic field of $B_0 = 7.04$ T are presented in Fig. 2 a-c. Due to the spectral width the measurements have to be done using the point-to-point method with selective excitation of small spectral windows to avoid signal distortions. The width of the signals decreases from the K to the Cs

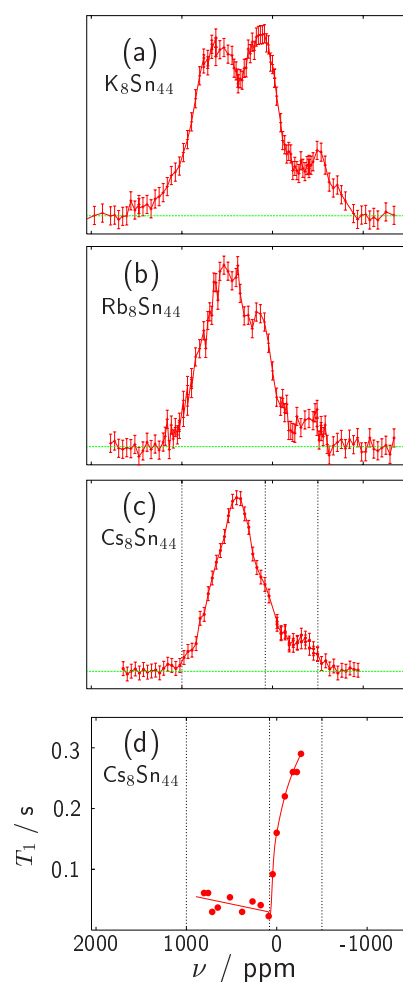


Fig. 2: (a-c) ^{119}Sn NMR spectra of $M_8\text{Sn}_{44}\text{I}_2$ with $M = \text{K}, \text{Rb}, \text{Cs}$. (d) frequency dependence of the spin-lattice relaxation time T_1 in $\text{Cs}_8\text{Sn}_{44}\text{I}_2$. The full lines represent a guide to the eye. The symbols in the spectra represent the integrated intensity of selective Hahn echo experiments.

compound. All three spectra have a three- or four-peak structure with different peak intensities. Nevertheless, the complex line shape prevents an assignment of the individual signal components.

A special feature of the NMR signals for $M_8\text{Sn}_{44}\text{I}_2$ with $M = \text{K}, \text{Rb}, \text{Cs}$ is the extremely large broadening of the peaks. Magic angle spinning (MAS) experiments were performed on $\text{Cs}_8\text{Sn}_{44}\text{I}_2$ to reduce the broadening and to determine the centers of gravity for shift assignment of the individual signals. These measurements result in no significant changes compared to the static spectrum. For nuclei without quadrupole moment only inhomogeneities of the sample and/or distributions of chemical shifts or Knight shifts can produce such an effect.

To investigate the origin of the shift distributions spin-lattice and spin-spin relaxation measurements were done and are still in progress. The frequency dependence of the spin-lattice relaxation time T_1 of ^{119}Sn in $\text{Cs}_8\text{Sn}_{44}\text{I}_2$ measured by selective saturation Hahn echo experiments is shown in Fig. 2 (d). The small frequency range of the signal shows significantly slower relaxation which indicates the non-equivalence of the atoms contributing to this part of the signal with respect to the other part of the signal.

Spin-spin relaxation measurements show a long T_2 compared to the spectral width of the signal. The natural width of the signal (T_2^*) calculated by assuming dipolar coupling dominates the signal and is in the order of the measured T_2 . This is an evidence for an inhomogeneous NMR signal. Hahn echo experiments with increasing distance (τ) of the $\pi/2 - \tau - \pi$ pulses (ensuring the signal-to-noise ratio of different spectra is nearly equal) show also different parts of the signal. This can be seen in the differences of both spectra presented in each sub-figure of Fig. 3 (a-c).

At present two competing models describing the spectra are under consideration:

- The signal is due to three or four groups of chemical or Knight shifts corresponding to the different positions Sn1, Sn2, and Sn3 (Sn31 and Sn32).
- The signal consists of a wide distribution of chemical or Knight shifts having the origin in slightly different positions of Sn1, Sn2, and Sn3 (Sn31,

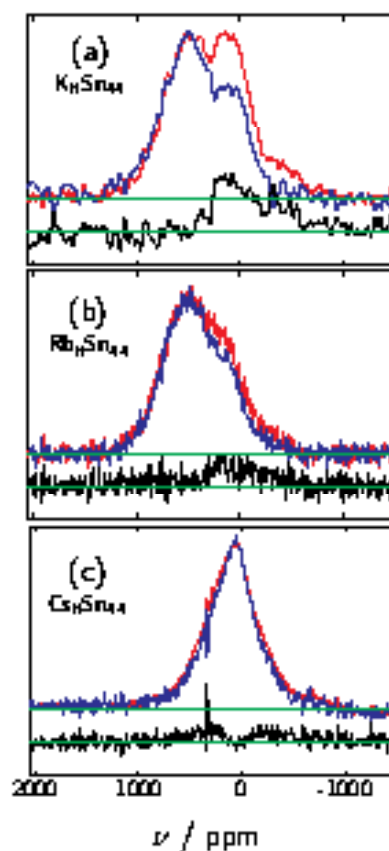


Fig. 3: Spin-spin relaxation of the ^{119}Sn signal of $M_8\text{Sn}_{44}\text{I}_2$ with $M = \text{K}, \text{Rb}, \text{Cs}$. The red lines represent the spectra with short spin-spin relaxation, the blue lines represent the spectra with advanced spin-spin relaxation. The black lines indicate the difference of both spectra.

Sn32) and of a broad asymmetric spectrum which is due to the anisotropy of the chemical shielding tensor caused by the lone pair of electrons located at Sn3 (Sn32) atoms neighboring a vacancy in the Sn1 position.

References

- [1] M. Baitinger, Dissertation, Technische Universität Darmstadt (2000).
- [2] G. S. Nolas, B.C. Chakoumakos, B. Mahieu, G. J. Long, T. J. R. Weakley, Chem. Mater. **12**, 1947 (2000).

^{11}B NMR of $\text{Al}_{0.9}\text{B}_2$

Ulrich Burkhardt, Vladimir Gurin, Frank Haarmann and Yuri Grin

Nuclear magnetic resonance (NMR) of nuclei with a quadrupole moment ($I > 1/2$) is sensitive to the electric field gradient at the examined positions. Lattice distortions, which are due to atomic disorder or other defects of a crystal, have a great influence on the electric field gradient and lead to a broadening of the satellite transitions whereas the central transition is not affected according to first order perturbation theory [1].

X-ray diffraction experiments and measurements of the mass density of aluminum diboride $\text{Al}_{0.9}\text{B}_2$ lead to a defect structure model with vacancies at the Al site. The composition determined by these experiments is $\text{Al}_{0.9}\text{B}_2$, even for single crystals grown from a melt of composition Al:B = 49:1.

The ^{11}B isotope has a small quadrupole moment and the experiments were done using a magnetic field of $B_0 = 7.04$ T. Therefore, first order perturbation theory is appropriate to analyze the data. In addition, ^{11}B has a high sensitivity for NMR experiments. The electric field gradient at the B site is determined by the covalent B-B bond and the coordination of the Al atoms (Fig. 1). A vacancy at a position of an Al atom produces a significant change of the electric field gradient at the B site compared to full occupation of all Al sites. Moreover, a relaxation of the lattice due to the influence of the vacancies can be expected. These will also influence the electric field gradients of neighboring positions.

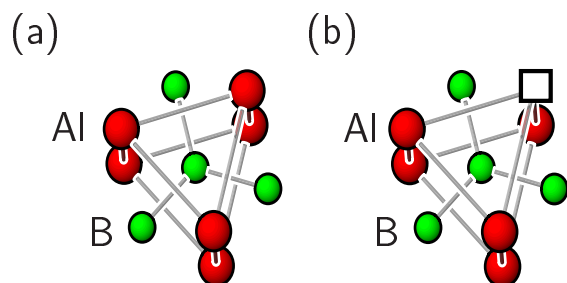


Fig. 1: Coordination polyhedra of B: (a) ideal and (b) one of the real configurations (\square = vacancy).

An ^{11}B NMR spectrum centered at a frequency of $\nu_0 = 96.26$ MHz is presented in Fig. 2a. The central transition was detected without distortions due to the measurement technique within a single Fourier transform spectrum. To measure the whole signal of such a broad spectrum without artifact, selective excitation of a narrow spectral window must be done using a Hahn echo sequence with low-power pulses of long duration. The whole spectrum is achieved by sweeping the frequency point by point.

The quadrupole frequency $\nu_Q = 540$ kHz \pm 20 kHz determined by least squares fitting of the spectrum is in good agreement to earlier results [3,4]. A slight asymmetry of the central transition is due to an anisotropy of the Knight shift which can be estimated to $\Delta K \approx 130$ ppm. Such an anisotropy has been predicted by *ab initio* calculations. The absolute value of the Knight shift of $K = -10.5$ ppm was determined in magic angle spinning (MAS) experiments [4]. The asymmetry param-

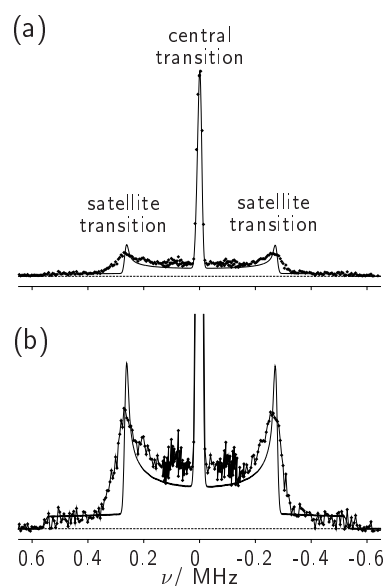


Fig. 2: ^{11}B NMR spectrum of $\text{Al}_{0.9}\text{B}_2$: \diamond selective excitation Hahn echo experiments; full line: calculated spectrum for $I=3/2$ with $\nu_Q=540$ kHz, $\eta_Q=0$, $\Delta K=130$ ppm, $\eta_K=0$. (b) Magnification of subfigure (a).

ters of quadrupole coupling and Knight shift can be neglected ($\eta_Q \approx \eta_K \approx 0$). This result is also obtained by a least-squares fit of the spectrum.

A broadening of the satellites with respect to the central transition is obvious (Fig. 2b). For a better comparison, a calculated profile is added to the figure. The broadening of the satellites is due to a distribution of quadrupole frequencies which most likely result from the influence of the vacancies at the Al sites. Thus, the results of our NMR experiments are in agreement with the model derived from X-ray diffraction data and mass density measurements [2].

References

- [1] *M. Mehring and O. Kanert*, Z. Naturforsch. **24a**, 332 (1969).
- [2] *U. Burkhardt, V. Gurin, F. Haarmann, H. Borrmann, W. Schnelle, A. Yaresko and Yuri Grin*, J. Solid State Chem. 2003 in press and Development of the Institute and Scientific Report "Aluminium diboride" MPI CPfS (2000).
- [3] *J. P. Kopp and R. G. Barnes*, J. Chem. Phys. **54**, 1840 (1971).
- [4] *S. H. Baek, B. J. Suh, E. Pavarini, F. Borsa, R. G. Barnes, S. L. Bud'ko and P. C. Canfield*, Phys. Rev. B **66**, 104510 (2002).

$^{71,69}\text{Ga}$ NMR Spectroscopy of Transition-Metal Monogallides

Annegrit Rabis, Rainer Giedigkeit, Frank R. Wagner, Andrei A. Gippius*, Michael Baenitz and Yuri Grin

The two „twin isotopes“ of gallium ($^{71,69}\text{Ga}$ with nuclear spin of 3/2 and abundance of 60.4 % and 39.6 %, respectively) were used as local probe to detect structural information in a series of binary gallides TMGa ($\text{TM} = \text{Ni}, \text{Pd}, \text{Pt}$). The NMR line shape of gallium containing materials and the position of the center of gravity are strongly dependent on the electric field produced by the environment (Electric Field Gradient, EFG). It is known that strong quadrupolar interaction causes very broad spectra. Due to the fairly high quadrupolar moment of both isotopes, the quadrupolar interaction is very often large, so that the $-3/2 \leftrightarrow -1/2$ and $1/2 \leftrightarrow 3/2$ transitions do not occur in the same spectral window as the main transition which is itself broadened by second order quadrupolar interaction. The main transition may reach several MHz in linewidth. Because of the lower quadrupolar moment, the higher resonance frequency and sensitivity, ^{71}Ga is the favorite nucleus. Furthermore, it is a very advantageous situation to have two NMR active isotopes to ensure the experimental results and the simulations as well. Therefore, we measured the resonance signals for both isotopes.

NiGa

NiGa crystallizes in the cubic CsCl structure. Due to the cubic site symmetry O_h of Ga atoms, no quadrupolar contributions are expected. The ^{71}Ga static powder pattern at room temperature is observed at a Knight shift $K = 0.206(5)$ %. In the MAS spectra with a maximal rotation frequency of 12 kHz the linewidth remains constant. Because of the weak Pauli-paramagnetic character of NiGa we can exclude an influence from magnetic moments of Ni on the linewidth. Therefore, it can be assumed that the linewidth is caused by a distribution of shifts, due to small disorder effects. The phase NiGa has a large homogeneity range [1] and the occurrence of substitutional disorder is known even for the equimolar composition [2]. By this effect the environment of some Ga atoms is changed. This causes small alterations of the

Knight shift and gives rise to tiny quadrupolar interactions, leading to the broadening of the NMR signal both in the static powder pattern and in the MAS spectrum. The temperature dependent ^{71}Ga and ^{69}Ga NMR spectra show a small shift to higher frequencies with higher temperatures. The signal widths decrease with increasing temperature, as expected.

PdGa and PtGa

PdGa and PtGa crystallize in the FeSi structure type with the space group $P2_13$ [3, 4]. The FeSi structure can be described as a strongly distorted NaCl variant with an increase of the coordination number from 6 to 7 for both atom types (Fig. 1) [5]. In the crystal structures of PdGa and PtGa, the shortest distances between transition metal and gallium occur along the three-fold axes: $d(\text{Pd-Ga}) = 254$ pm and $d(\text{Pt-Ga}) = 257$ pm (from our X-ray single crystal structure refinements).

Due to the C_3 symmetry of the Ga site and the influence of the short distance mentioned above, the NMR spectra are dominated by second order quadrupolar interactions. The ^{71}Ga point-by-point NMR spectrum at 4.2 K of PdGa including the

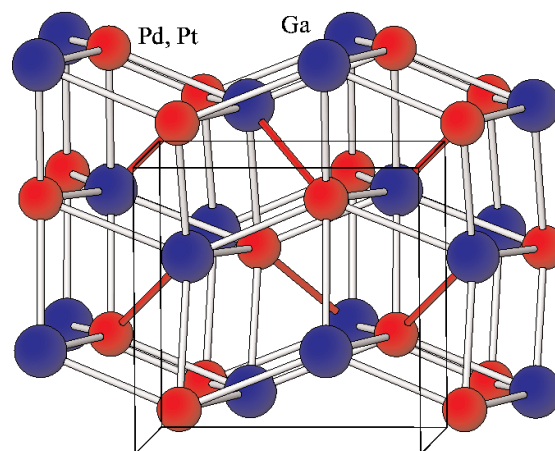


Fig. 1: Crystal structure of PdGa and PtGa, respectively. The shortest distances along the three-fold axes are marked red.

satellite transitions is presented in Fig. 2 together with the signal observed for the main transition. The Knight shift $K = 0.304(10) \%$ is positive and close to the one observed for a Pd(Ga) alloy with 5 % gallium ($K = 0.320(10) \%$ [6]). Also of interest is also the fairly large quadrupolar interaction resulting in a quadrupolar coupling constant $\nu_{\text{NQR}} = 16.6(2) \text{ MHz}$. It points to a high EFG at the gallium site and supports the finding of a strong lattice distortion detected by X-ray diffraction. Using the general equation $|V_{zz}| = \nu_{\text{NQR}} h/eQ$ an EFG $|V_{zz}^{\text{Ga}}(\text{PdGa})| = 7.14 \times 10^{21} \text{ V/m}^2$ was obtained. For PtGa the observed Knight shift $K = 0.197(10) \%$ and the quadrupolar coupling constant $\nu_{\text{NQR}} = 14.1(2) \text{ MHz}$ are smaller than for PdGa. From this quadrupolar coupling constant an electric field gradient $|V_{zz}^{\text{Ga}}(\text{PtGa})| = 6.04 \times 10^{21} \text{ V/m}^2$ is derived. First principles electronic structure calculations for the experimentally determined crystal structure on the scalar-relativistic DFT level using the full potential APW+lo code WIEN2k [7] resulted in electric field gradients $V_{zz}^{\text{Ga}}(\text{PdGa}) = -5.8 \times 10^{21} \text{ V/m}^2$ and $V_{zz}^{\text{Ga}}(\text{PtGa}) = -5.0 \times 10^{21} \text{ V/m}^2$. A calculation of PtGa using the structural parameters of PdGa resulted in the same value V_{zz}^{Ga} , indicating that the different EFGs are primarily caused by structural differences. Structural relaxation has a significant influence on these values and test calculations indicated an up to 20 % decrease by just optimizing the internal parameters at the experimental lattice con-

stants determined at $T = 293 \text{ K}$. Taking this into account, the agreement with the NMR experiment (at $T = 4.2 \text{ K}$) is satisfactory.

Summary

Investigations of binary transition metal monogallides TMGa ($\text{TM} = \text{Ni}, \text{Pd}, \text{Pt}$) have shown that gallium NMR is a sensitive local probe to extract the structure information as well as the electrical environment and provides information which cannot be found with other methods. The Knight shifts found here are in a good agreement with literature data observed for palladium-rich alloys. It could be demonstrated that the value of the quadrupolar coupling constant is sensitive to small structural changes. A significantly smaller value has been found for PtGa in comparison to PdGa. With the knowledge of the quadrupolar coupling constants ν_{NQR} the absolute values of the EFG can be derived. These values are in a good agreement with those found by theoretical calculations which additionally provide the algebraic sign. On the other hand, knowledge of experimental EFGs for a system under study represents a valuable information for the evaluation of the quality of certain approximations used in a quantum mechanical calculation.

References

- [1] E. Hellner, Z. Metallkd. **41**, 480 (1950).
- [2] K.-J. Best, Z. Metallkd. **62**, 419 (1971).
- [3] E. Hellner, F. Laves, Z. Naturforsch. **2a**, 177 (1947).
- [4] M. K. Bhargava, A. A. Gadalla, K. Schubert, J. Less-Common Met. **42**, 69 (1975).
- [5] L. Pauling, A. M. Soldate, Acta Crystallogr. **1**, 212 (1948).
- [6] G. A. Matzkanin, D. O. van Ostenburg, J. J. Spokas, H. G. Hoeve, C. H. Sowers, Bull. Am. Phys. Soc. **13**, 363 (1968).
- [7] P. Blaha, K. Schwarz, G. K. H. Madsen, D. Kvasnicka, J. Luitz, Computer code WIEN2k, An Augmented Plane wave + Local Orbitals Program for Calculating Crystal Properties, Wien2k (Karlheinz Schwarz, Technische Universität Wien, Austria, ISBN 3-9501031-1-2).

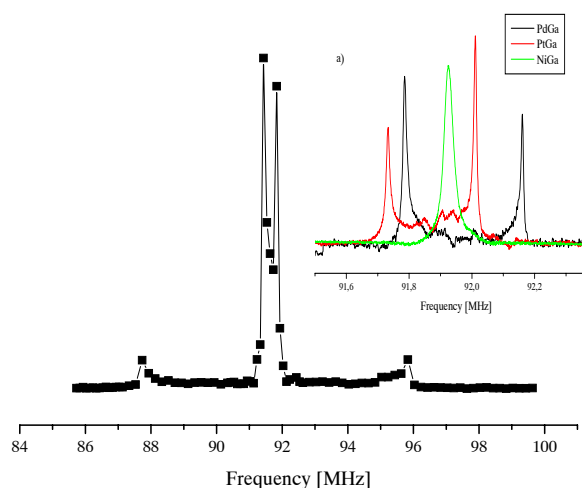


Fig. 2: ^{71}Ga -NMR spectrum for PdGa at 4.2 K, inset: central transition for NiGa, PdGa, PtGa.

* Moscow State University, Faculty of Physics, 119899 Moscow, Russia